Received: 7 September 2022 | Revised: 17 January 2023 | Accepted: 20 January 2023

DOI: 10.1002/oa.3206

RESEARCH ARTICLE

Defects-related early childhood caries as hints of possible maternal–fetal health issues: Evidence from medieval northern Italy

Chiara Tesi[1] | Stefano Ricci[2] | Luca Levrini[3] | Giovanna Giorgetti[4] | Monica Campagnolo[5] | Rosagemma Ciliberti[6] | Roberta Fusco[1] | Omar Larentis[1] | Marta Licata[5]

[1]Centre of Research in Osteoarchaeology and Paleopathology, Department of Biotechnology and Life Sciences, University of Insubria, Varese, Italy

[2]Research Unit in Prehistory and Anthropology, Department of Physical Sciences, Earth and Environment, University of Siena, Siena, Italy

[3]Department of Human Sciences, Innovation and Territory, University of Insubria, Varese, Italy

[4]Department of Physical Sciences, Earth and Environment, University of Siena, Siena, Italy

[5]Department of Biotechnology and Life Sciences, University of Insubria, Varese, Italy

[6]Section of History of Medicine and Bioethics, Department of Science of Health, University of Genoa, Genoa, Italy

Correspondence
Roberta Fusco, Centre of Research in Osteoarchaeology and Paleopathology, Department of Biotechnology and Life Sciences, University of Insubria, Varese, Italy.
Email: roberta.fusco@uninsubria.it

Funding information
Regione Lombardia; Fondazione Cariplo; Fondazione Comunitaria del Varesotto

Abstract

Developmental defects of enamel (DDE) are important markers of stress as they arise from the disruption of ameloblastic activity during enamel matrix secretion and mineralization. Defects on the crowns of the deciduous dentition provide insights into maternal–fetal health because they can emerge during intrauterine development as a result of gestational issues. The presence of previous defective enamel represents one of the most predisposing causes of caries development. Thus, circular caries on the deciduous dentition are considered an indicator of stress because of their ascertained relation with dental enamel defects. In bioarchaeological analysis, these lesions allow us to deepen the question of maternal–fetal health issues in the ancient period. Here, we present evidence of defects-related early childhood caries in three infants from a medieval cemetery in northern Italy. The findings in the dentitions of the three subjects were investigated with a multi-analytical approach, including macroscopic examination, microscopic observation, cone-beam computed tomography (CBCT), scanning electron microscopy (SEM), and histological sections. In the specimens analyzed, the lesions observed in the dentitions appeared to have arisen during the fetal period and then protracted in the postnatal life, suggesting the implication of in utero environment and maternal health in the etiology of defects.

KEYWORDS
bioarchaeology, circular caries, deciduous dentition, enamel defects, gestational stress, rampant caries

1 | INTRODUCTION

Dental disorders are considered indicators of general health since changes involving dental tissues provide information on individuals' nutritional status and social context (Madhusudhan & Khargekar, 2020).

Studies on current disadvantaged populations, where children live in unhealthy environments characterized by scarcity of food resources, have shown that tooth growth and eruption are stable biological processes whose timings only marginally suffer from extreme conditions of stress and malnutrition (Elamin & Liversidge, 2013). Similarly, investigations on a sample of modern immature skeletons from the Lisbon

identified skeletal collection have revealed that dental development is less influenced by environmental factors than skeletal growth (Conceição & Cardoso, 2011). Nevertheless, if tooth size and timing of emergence are only slightly biased by negative events that occurred during the period of formation, qualitative and quantitative aspects of enamel and dentin can undergo changes if their cellular activity is perturbed by endogenous or exogenous insults (Jacobsen et al., 2013).

Developmental defects of enamel (DDE) are important markers of stress as they originate from a cellular disruption of ameloblasts during tooth formation (Lang et al., 2016). Because dental enamel is not subject to remodeling after deposition and mineralization, any disturbance that occurs during its development remains permanently recorded on the dental crown surface (Lacruz et al., 2017), proving to be the best chronologic recorder of negative events (Caufield et al., 2012; Velló et al., 2010).

According to the modified DDE index (Clarkson & O'Mullane, 1989; FDI, 1992), defects can be classified into three major categories: hypoplasia, opacities (or hypocalcifications), and discolorations. Hypoplasia (EH) is a quantitative defect manifested as decreased localized enamel thickness resulting from disorders during the secretion phase of the enamel matrix. The hypoplastic defects may vary in form of furrows, pits, or planes of enamel thickness deficiency (Schroth et al., 2021). Hypocalcifications are expressed as opaque white patches in the translucent enamel, in form of demarcated or diffuse opacities, caused by disruption at the maturation stage (Aminabadi et al., 2009; Castro et al., 2021). Discolorations are deposits of pigments as a result of disorders during the mineralization phase (Hillson, 2014). Disruptions may result in different outcomes depending on the stage of enamel formation involved, the extent and duration of the insult, and the exposure to causative factors. Defects may affect primary as well as permanent dentition, depending on the time frame of insult experienced (Jacobsen et al., 2013).

Because of their distinctive developmental pattern and stable metabolic structure, deciduous teeth act as event recorders during early growth from gestation until the end of the first year of life (Levine et al., 1979). In fact, the onset of formation of primary teeth starts during intra-uterine life so that, at the time of birth, all stages of tooth development are present. Approximately, at the 13th week of gestation, the deciduous maxillary central incisors develop, and, at birth, the entire crown of these teeth appears almost completely formed, but only the incisal margin presents whole mineralization while the surrounding enamel is at the pre-eruptive maturation phase (Mjor & Fejerskov, 1986). The other primary teeth begin to develop from the 15th week with a phase shift of a few weeks from each other (Hillson, 2014). Completion of the crown formation and maturation occurs in the perinatal and postnatal period, by 9–11 months from birth (canine, second molar) (Reed et al., 2017). Insults that occurred during this interval can permanently impair the primary enamel, providing a chronological indicator of the stressful events. Therefore, defects of primary teeth are often suggestive of diseases and dysfunctions suffered by the mother and the fetus during pregnancy (Aminabadi et al., 2009; Cook & Buikstra, 1979).

DDE are considered in several clinical studies (Caufield et al., 2012; Schroth et al., 2021) to be the major predisposing factor to early childhood caries (ECC) onset, as they compromise the structural integrity of teeth (Enwonwu, 1973).

Paleopathological cases of ECC are numerous and have recorded an increase of deciduous caries in the postmedieval period compared with the previous times (Moore & Corbett, 1973; Lewis, 2013).

Some authors have found severe early childhood caries (S-ECC) associated with underlying DDE, often assuming a probable co-cause consisting of a carbohydrate-rich and cariogenic diet, and others suggested the use of pacifiers or feeding bottles as a possible cause of rampant caries in early childhood, perhaps suffering from some diseases for which they often needed to be comforted (Lewis, 2017).

A possible case of baby bottle caries was reported from Late Roman Ancaster, England (Bonsall et al., 2016), in a subadult aged 3–4 years presenting severe circular caries to all deciduous teeth. Walker (2012) provided a case of a child from postmedieval Bunhill in London with extensive caries on anterior deciduous teeth, suggesting a severe deep plane enamel hypoplasia and superimposed decaying. Several cases of early caries from the medieval and postmedieval site of St Oswald's Priory, Gloucester (Lewis, 2013), suggest susceptibility of children to ECC because of environmental growth conditions and maternal stress.

The present paper deals with the detection of severe defects of the dental enamel in three subadult individuals unearthed during the archaeological investigations of the medieval and postmedieval cemetery of San Biagio in Cittiglio (Lombardy, northern Italy). This study aims at illustrating this pathological disorder in the light of a significant presence of infantile individuals in the investigated sample and at drawing attention to its potential as a source of information on the nourishment and living conditions of children in the past.

2 | MATERIALS AND METHODS

2.1 | The archaeological site

The medieval church of San Biagio in Cittiglio and its related cemetery areas have been investigated since 2006. The religious building represents a typical Romanesque example, but its origin can be traced in the Early Middle Ages. During the centuries, the church has undergone several architectural modifications discovered by archaeological excavations conducted inside and outside the church revealing phases of funerary use dating from the 10th to the 17th centuries. Several archaeological campaigns conducted between 2006 and 2020 have made it possible to bring to light 22 burials and a common ossuary, inside the church, and 61 tombs and a large common ossuary in the external area (Licata et al., 2019).

2.2 | Materials

Among the tombs of the external area, three subadults showed pathological lesions affecting the deciduous dentition (T.43, T.72, Mx1-SU423). Age-at-death estimations of the three individuals are reported in the results section.

The skeleton of Tomb 43 dated between the 14th and 15th centuries. The burial was characterized by the presence of grave goods,

an iron buckle, and several beads located in the thoracic–cervical region, probably pertaining to a funerary dress. The skeleton was not in an excellent state of conservation, and few anatomical parts were represented. Maxillary bone was preserved only in a few fragments, and the mandible was present although not complete. Dental elements preserved consisted of the entire maxillary and mandibular deciduous dentition, except for both lower canines (Figure 1).

The skeleton of Tomb 72 dated between the 13th and the 14th centuries. The skeleton was partially preserved. The cranium and the upper portion of the skeleton were present up to the lumbar trait. The maxilla and mandible appeared complete and well preserved. All the deciduous mandibular teeth and part of the maxillary dentition (molars and incisors) were recovered (Figure 2).

The individual Mx1-SU423 coming from the external ossuary was represented only by the maxilla and the relative deciduous dentition, together with some elements of the permanent dentition protected inside the bone crypts. Deciduous molars of both sides and the right lateral incisor were recovered (Figure 3). The maxillary bones came

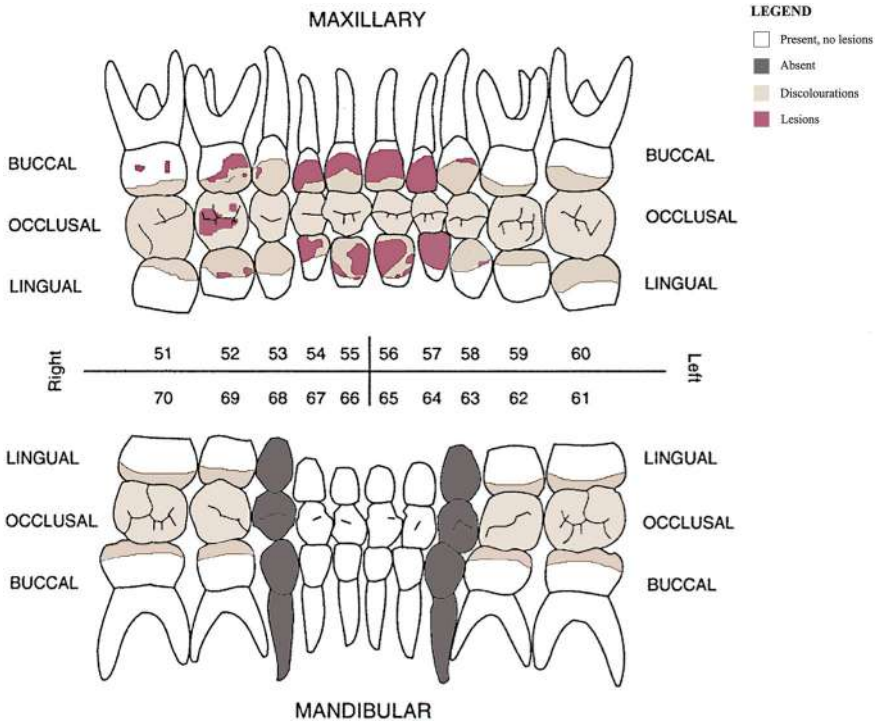

FIGURE 1 Preservation of T.43 and distribution of dental lesions: Preserved teeth are marked in white, pink areas indicate the enamel and dentin lesions, and light brown displays the areas of discolorations (image: modified from Buikstra and Ubelaker, 1994, attachment 14b). [Colour figure can be viewed at wileyonlinelibrary.com]

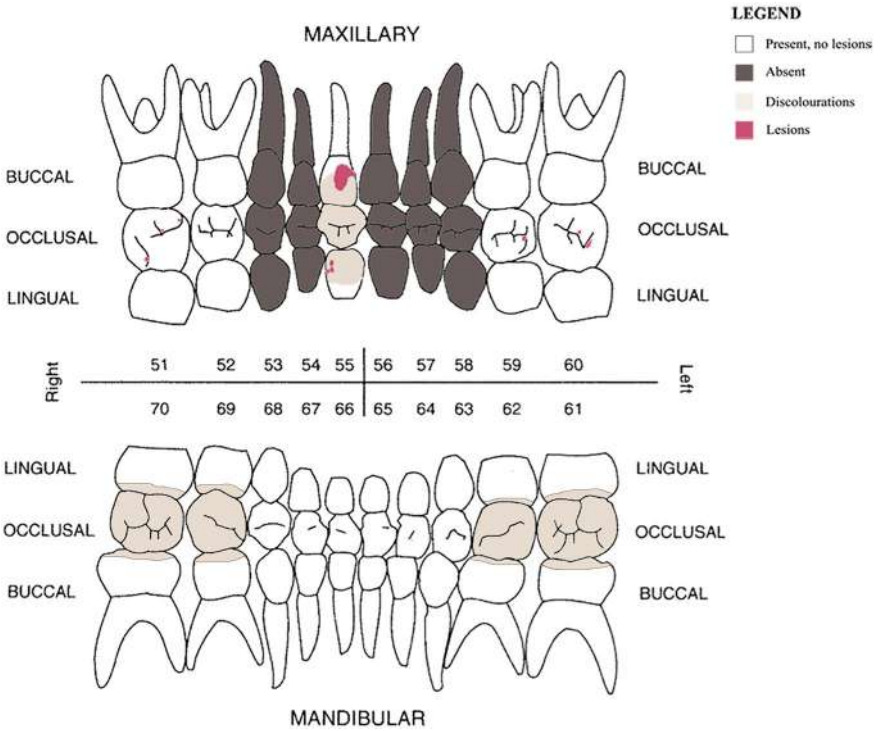

FIGURE 2 Preservation of T.72 and distribution of dental lesions: Preserved teeth are marked in white, pink areas indicate the enamel and dentin lesions, and light brown displays the areas of discolorations (image: modified from Buikstra and Ubelaker, 1994, attachment 14b). [Colour figure can be viewed at wileyonlinelibrary.com]

from the excavation of the large ossuary pit SU 423, located on the eastern border of the external churchyard area. The realization of the pit presumably represented the last cemetery phase, placed in modern times probably after 1632, when, according to documentary sources, the funerary activity in the churchyard ceased. In fact, dating elements were retrieved inside the ossuary such as votive medals and rings that allowed us to date the burials to a postmedieval period.

2.3 | Methods

Skeletal remains were macroscopically analyzed to determine the biological profile, and all the bones were observed to record any pathological changes. Age-at-death of the immature remains was estimated from the degree of teeth mineralization (AlQahtani et al., 2010; Liversidge et al., 1998). Given the immaturity of the subjects, no attempts at determining the sex have been conducted.

Dental elements of the three individuals were first macroscopically observed, and pathological changes affecting teeth were subsequently photographed in detail. All the teeth were examined for defects using magnification and oblique lighting and rotating the teeth at various angles to permit the visualization of areas of defective enamel. The position of the defects on the crown surface was recorded using a digital caliper, measuring the distance between the cemento-enamel junction (CEJ) and the cervical and occlusal margins of the lesion.

A standard reflected light optical microscope was used for microscopic observation of the affected teeth of all the individuals, at a level of magnification of 20×.

!Subsequently, a cone-beam computed tomography (CBCT) was performed in Como (Brenna and Levrini dental practice). Scans were conducted on both arches of the individual of T.43, as this specimen presented the greatest number of dental lesions compared with the other subjects. Conventional dental radiological equipment was used (NewTom GiANO HR). Imaging parameters were as follows: 90 kV, 3 mA. The slice thickness used was 0.3 mm, and the voxel size was 75 µm. To compare the radiodensity of the different dental tissues, high-resolution scans and 3D reconstruction of the dental arches were performed.

Scanning electron microscopy (SEM) was carried out on the samples for the detailed micro-observation of the surface topography at the Department of Physical Sciences, Earth and Environment of the University of Siena. Two teeth of the individual from T.43, the maxillary left lateral incisor and the right upper canine, were selected for the analysis. A Philips XL30 operating at 20 kV and equipped with an EDAX-DX4 energy dispersive spectrometer (EDS) was used. Prior to the observation under SEM, the sample was carbon coated (∼10 nm) to provide good-quality images. As to exclude the carbon cover component from the EDS analysis of the dental enamel, a second SEM observation was conducted with different teeth at the Unitech Office, University Technology Platforms of the University "Statale" of Milan, coating the samples with a subtle layer of gold with a Sputter Nanotech (Assing) prior to the observation under an LEO 1430 scanning electron microscope. The upper right first molar and the right maxillary incisor of the individual from T.43 were chosen for this second observation. Simultaneously with the second observation, a deciduous upper canine with apparently sound enamel from another individual of the sample was used as a comparison. Moreover, energy-dispersive X-ray spectroscopy (EDS System) was performed to evaluate the ion content in different points of the enamel of the affected teeth and of an apparently sound tissue from the comparison sample.

Finally, histological section preparation and observation were conducted in the orthopedics and plastic surgery laboratory of the University of Insubria to evaluate the microscopic aspect of hard tissues affected by the lesions. For these observations, the upper central incisors of T.43 were chosen, which presented some of the most consistent lesions among all those observed in the affected subjects. In total, four thin sections were obtained, two for each incisor, of which two were decalcified and two undecalcified. The teeth were subjected to longitudinal thin sections up to a thickness of 4 µm for the decalcified and 100 µm for the undecalcified sections, according to the procedure detailed below (see histological processing of teeth). The thin sections were observed with Leitz Aristoplan optical microscope at 10× and 25× under normal light and polarized light (POLMI).

The dentition of one of the three individuals under study (T.43) was subjected to complete analyses, necessarily having to sacrifice part of the surviving teeth, and the affected dental elements of the other two subjects (T.71, Mx1-SU423), which have a similar appearance, were observed macroscopically and microscopically to preserve their completeness and integrity.

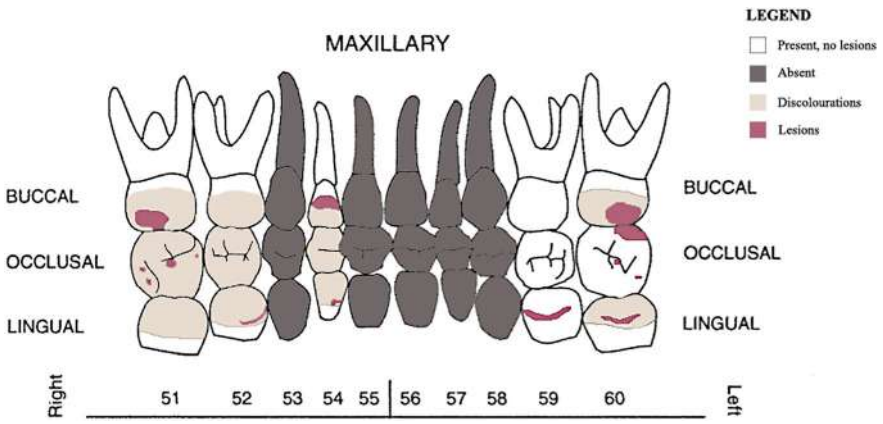

FIGURE 3 Preservation of Mx1-SU423 and distribution of dental lesions: Preserved teeth are marked in white, pink areas indicate the enamel and dentin lesions, and light brown displays the areas of discolorations (image: modified from Buikstra and Ubelaker, 1994, attachment 14b). [Colour figure can be viewed at wileyonlinelibrary.com]

Enamel defects, according to the modified DDE index chart (Clarkson & O'Mullane, 1989), were recognized as hypoplasia, discoloration, and opacities, observing the eventual presence of opaque patches, circular bands of yellow-brown discolored enamel, and irregularities of the surface in form of pits, furrows, and planes of thinning or missing enamel.

Age at the formation of defects has been hypothesized by observing their localization in the crown, referring to the table of development of deciduous teeth by Lunt and Law (1974), Liversidge and colleagues (1993), and Hillson (2009) and to the tooth developmental data from autopsied infants by AlQahtani et al. (2010). Moreover, we referred to metric data and plots of tooth length from Irurita et al. (2013), Minier et al. (2014), and Cardoso et al. (2019) to estimate the stage of tooth formation and derive information on the development of defects before or after birth.

2.4 | Histological processing of teeth: Undecalcified sections

The area of greatest interest of the tooth was chosen and subjected to two parallel cuts to obtain a section 5 mm thick. The samples were cut with a diamond band saw (EXAKT 300 CP, Exakt Technologies, Germany). Then, the sections obtained were subjected to a slow dehydration process, which involved baths in distilled water and ethanol solutions with increasing concentrations of up to 100% absolute ethanol. After that, the sample was infiltrated with photopolymerizable methacrylate-based resin (Technovit 7200). The final resin embedding was photopolymerized in a UV lamp (EXAKT 520, Exakt Technologies, Germany).

From the solidified resin block containing the sample of interest, some sections reduced to about 100 μm in thickness were obtained through the EXAKT abrasion unit, which involved the use of increasingly fine-grained abrasive papers.

2.5 | Histological processing of teeth: Decalcified sections

The tooth sample was decalcified using Bio-Optica's rapid Biodec for a week, once the elastic consistency of the sample was ascertained. After the decalcification, the sample was rinsed to remove any residue, and then we proceeded with the dehydration process. After that, the clarification through Bio-Optica's BioClear was performed, and the sample was included in paraffin.

The paraffin block was then subjected to microtome cutting to obtain slices with a thickness of about 4 μm with which the slides were prepared. The decalcified tooth slices were subjected to two types of staining:

1. hematoxylin–eosin, which colors the acid (hematoxylin solution) and basic substances (eosin).
2. toluidine blue-basic fuchsin, which colors acidic (toluidine blue) and basic tissue components (fuchsin).

3 | RESULTS

The remains from T.43, T.72, and Mx1-SU423 belonged to three subadults respectively aged between 18 months and 2 years old, 3 and 4 years old, and 2 and 2.5 years old.

Preserved dental elements and those displaying pathological changes are graphically shown in Figures 1–3. Pathological evidence was observed in the oral region, affecting the deciduous dentition with different degrees of severity. The involvement of dental crowns, albeit in different amounts, seemed to present similar features.

In Table 1, the measurements indicating the position of the lesions on the crown surface for each tooth have been recorded.

The three cases were analyzed separately, and for T.43, some teeth were subjected to destructive analyses for further tests: In particular, the upper central incisors were selected for decalcified and undecalcified histological analyses, and the maxillary lateral incisors, the upper right canine, and the upper right first molar were collected for the SEM observations.

The results of the three specimens are detailed below.

3.1 | Tomb 43

On the first examination, most of the maxillary teeth appeared to be affected. Maxillary anterior teeth showed wide circumferential bands of enamel loss, which interested seamlessly all the surfaces of the crowns, circling around and forming a continuous defect. Loss and changes of the underlying dentin were extensive. Posterior teeth showed less involvement; nevertheless, also in the molars, the alterations were evident although not generalized. Between all surfaces, the labial and lingual sides of the anterior teeth and the occlusal and buccal ones of the molars were more seriously impaired (Table 2). Preserved enamel, in general, was found in the cervical region and showed sharp and irregular margins and undercut edges toward the areas of defects. It cannot be excluded that the irregular appearance of the enamel margins may also be the outcome of microfractures or microchippings of postdepositional origin.

Central incisors were characterized by huge bands of tissue loss, sparing the incisal and cervical region, which appeared to retain the original enamel. These crowns were eroded along a circumferential band affecting approximately the middle portion saving an inner part of the dentin, which appeared smooth and remodeled. The left lateral incisor (Ldi2) presented a similar appearance. The right lateral incisor (Rdi2) was almost destroyed by the lesions, as the tooth lost most of its volume and only the cervical portion of the crown was spared (Figure 4a).

In the posterior teeth, the most affected was the first right molar (Rdm1) being the buccal, mesial, lingual (Figures 4a and 5), and occlusal surfaces involved by extensive lesions. The discoloration extended to almost the entire crowns. Enamel loss and discoloration seemed to spare the cervical region, saving a narrow band of untouched enamel (Figure 4a).

As regards mandibular dentition, observable changes were expressed as discoloration of the crowns and a few slight enamel

TABLE 1 Measurement of the occlusal and cervical margins of the enamel lesions of each of the affected teeth, to indicate their position on the dental crown.

		R					L				
		dm2	dm1	dc	di2	di1	di1	di2	dc	dm1	dm2
T.43	Cervical		2.18		2.06	1.13	1.25	2.72	2.86		
	Occlusal		2.93			2.56	3.64	4.87	3.53		
T.72	Cervical					0.91					
	Occlusal					4.17					
Mx1-SU423	Cervical	2.48	2.25		1.08					1.78	2.27
	Occlusal	4.46	2.93		3.3					3.02	4.86

Note: The measurements shown, in millimeters, correspond to the distance of the margins of the lesion from the CEJ.

imperfections, visible in grazing light or microscopically. Areas of superficially pitted enamel were highlighted, especially on the buccal sides of the molars (Figure 4b).

In addition, the mandible appeared also affected by porosity and the deposition of a fine and porous layer of new woven bone (Figure 4b). Similar evidence was also observed in other skeletal districts such as on the ectocranial bones, the inferior surface of the pars basilaris, and on the diaphysis of long bones.

A detailed description of the dental lesions is shown in Table 2.

Cone-beam tomographic scans (Figure 6) revealed normally developed pulp chambers and roots and a normal degree of radiodensity between enamel and dentin.

Microscopic examination in reflected light allowed us to magnify the areas of lesion. The edges of preserved enamel appeared sharp, undercut, and irregular, characterized by little chippings and breakages. The cervical enamel was sound, without imperfections and discoloring or opacities.

In the first right maxillary molar, the surface of the occlusal opening was clearly observable: the cavity was wide and deep, and the dentin of the walls and floor was smooth and well remodeled. On the mesial and buccal surfaces, we observed areas in which enamel appeared irregular, pitted, opaque, and chalky white in color.

Undecalcified histological longitudinal sections of central maxillary incisors showed unusual early wear of the enamel at the incisal apex. Moreover, the images revealed a translucent appearance of the enamel interrupted by large, localized areas of tissue that returned a more opaque aspect, light brown in color. These areas were situated mainly near the tissue breakdown, both deeply and superficially to the enamel layer, and appeared bounded by an irregular dark line (Figure 7a). Under POLMI, the enamel appeared mostly translucent-light blue in color, interrupted by large opaque-white areas. Beneath enamel breakdown, extensive erosion associated with marked sclerosis and new formation of the underlying dentin were observed. In decalcified sections, thanks to the coloring with eosin and fuchsine, the appearance of dentin erosion and new formation, in the form of an area of tubules-rich tissue below the enamel breakdown, were particularly evident (Figure 8).

Enamel at SEM magnification showed areas of irregular topography and roughness, with cavities and irregularities near the area of breakage (Figure 9). The preserved surface was interrupted by a sharp breakdown exposing an underlying layer of irregular enamel (Figure 9b,c) and exposing wide areas of dentin (Figure 9a,d). Inside the breakdown of the tissue, a roughed topography was observed, with ridges of enamel alternated with irregular depressions (Figure 9b). In some crowns, the internal enamel layer uncovered by the tissue loss was interrupted with a rounded edge toward the areas of dentin exposure (Figure 9a).

Furthermore, SEM-EDS was performed to compare the ion content of the surface enamel at the yellow-brownish discolored region and the area of enamel breakdown in one affected crown (Ldi2), with the apparently normal enamel of a primary tooth from an individual of the same age.

The results of the analyses are illustrated in Table 3.

3.2 | Tomb 72

The first examination of the specimen revealed a picture of alterations of the dental enamel combined with some quite extensive lesions on the crowns involved. Of the preserved dentition, the right central maxillary incisor (Rdi1) appeared particularly affected. A wide and deep circular cavitation, which occupied a large portion of the surface, was observed on the labial side, sparing thin edges of incisal and cervical enamel (Figures 10c and 11b). A lesion was noted on the mesial side, with a second small circular cavitation near the incisal tip (Figure 10d). The lingual and distal surfaces were also affected, in the form of three circular defects coalescing into a single wider lesion along the distal border of the crown (Figure 10b). The molars showed pinpoint erosions in the intercuspal space (Figures 10a and 11a). These wide lesions presented irregular shapes and sharp margins and involved the underlying dentin that appeared eroded and deepened in the most severe cases.

Furthermore, observing the crowns microscopically and macroscopically in grazing light, it was observed that especially mandibular teeth were studded with small circular pitted defects both on the lingual and labial surfaces (Figure 12a,c,d). Some larger defects were also identified on a few crowns (Table 4; see the description of Rdi2 and Ldi2, Ldc, and Rdm1). These defects were characterized by superficial

TABLE 2 Detailed description of the dental lesions observed on T.43.

Tooth	Side	Surfaces	Defect type	Description
Maxilla				
di1	R	Labial, lingual, mesial, distal	Discoloration, enamel loss, dentin erosion	A wide labial band of enamel loss is located between the central third and the cervical third of the crown. On the lingual side, the defect continues seamlessly through both interproximal surfaces affecting much of the crown height on both sides. Dentin erosion has progressed to spare a small central portion. Brownish discoloration involves almost the entire crown, sparing a thin cervical band.
	L	Labial, lingual, mesial, distal	Discoloration, enamel loss, dentin erosion	A huge labial band of enamel loss affects most of the crown, sparing only the incisal and cervical portions. On the lingual side, the defect continues seamlessly through both interproximal surfaces, affecting a large part of the height of the crown, on the mesial portion. Brownish discoloration involves almost the entire crown, sparing a thin cervical band.
di2	R	Entire crown	Enamel loss, dentin erosion, crown destruction	Enamel loss and erosion of dentin affect the entire crown, sparing a narrow cervical band. Almost the entire crown is destroyed. A portion of dentin protrudes beyond the residual enamel, with evidence of tertiary closure of the pulp cavity.
	L	Labial, mesial, lingual	Discoloration, enamel loss, dentin erosion	Wide labial band of enamel loss, located between the central third and the cervical third of the crown. On the lingual side, the defect continues seamlessly through the mesial surface affecting much of the crown in the lingual portion along the mesial border. Brownish discoloration involves almost the entire crown, sparing a thin cervical band.
dc1	R	Labial	Discoloration, enamel loss	Loss of external enamel in the form of a small linear surface scratch. Brownish discoloration involves almost the entire crown, sparing a thin cervical band.
	L		Discoloration	Brownish discoloration affects almost the entire crown. A thin cervical band is spared.
dm1	R	Buccal, lingual, mesial, occlusal	Discoloration, enamel loss, dentin erosion	Multiple areas of localized enamel loss on the buccal, lingual, and mesial surfaces. The buccal surface is the most affected, with a large linear imperfection. Multiple small areas of defects are also detected on the lingual and mesial portions. On the occlusal surface, an extensive cavity with perforation of the enamel and erosion of the dentin is visible on the distal cusps; on the mesial side, a second small circular cavitation is present. Discoloration involves the occlusal third of the crown. Linear white opacities are observed along the discoloration borders.
	L	Buccal	Discoloration, enamel defects	Small areas of defect are visible on the buccal side. Brownish discoloration involves the occlusal third of the crown.
dm2	R		Discoloration	Brownish discoloration involves circumferentially the occlusal third of the crown.
	L		Discoloration	Brownish discoloration involves circumferentially the occlusal third of the crown.
Mandible				
dm1	R	Buccal	Enamel defects	Superficial pitted defects are observed on the buccal surface.
dm2	R	Buccal	Enamel defects	Superficial pitted defects are observed on the buccal surface.

Note: For each affected tooth, the side, surfaces, and type of defect are indicated.

FIGURE 4 Dentitions of T.43. (a) Deciduous maxillary teeth showing extensive erosive lesions to the enamel and dentin. The maxillary bones were not preserved. (b) Mandible of T.43 with preserved dental elements: On the buccal surfaces of the right molars, areas of superficially pitted enamel are observable. The scale bar equals 2 cm. [Colour figure can be viewed at wileyonlinelibrary.com]

FIGURE 5 Detail of the mesiolingual (on the left) and distobuccal (on the right) surfaces of Rdm1 of T.43. Lesions, areas of yellow-brown discoloration, and white-opaque areas are visible. The scale bar equals 1 cm. [Colour figure can be viewed at wileyonlinelibrary.com]

loss of enamel tissue, smooth and rounded borders, and exposure of circumscribed areas of underlying dentin, which appeared untouched (Figure 12c,d). Irregularities in occlusal enamel deposition were detected, together with early wear of the molars' cusps (Figure 12b). In this case, the brownish discoloration of the crowns was more subtle and was only slightly observed on the mandibular molars, mostly at the occlusal level.

In addition, the alveolar, maxillary, and palatal regions appeared affected by a widespread porosity and the deposition of a thin and porous layer of new bone (Figure 10a,b), as well as the inferior surface of the orbital cavity, the posterior portion of the zygomatic process, and the medial surface of the mandibular ramus (Figure 12b). Evidence of branched furrows was detected in the anterior surface of the maxilla, in the proximity of the infraorbital foramen (Figure 10c), and on the medial body of the mandible, along the mylohyoid line. Marked alveolar resorption with bowing of the alveolar borders and diffuse pitting were also recorded in the maxilla (Figure 10a,c). Similar evidence was also observed in other skeletal regions, such as in the endocranium.

A detailed description of the dental lesions is shown in Table 4.

FIGURE 6 Cone-beam tomographic scan: cross-section of the maxillary teeth of T.43. Enamel lesions of the crowns are observed. [Colour figure can be viewed at wileyonlinelibrary.com]

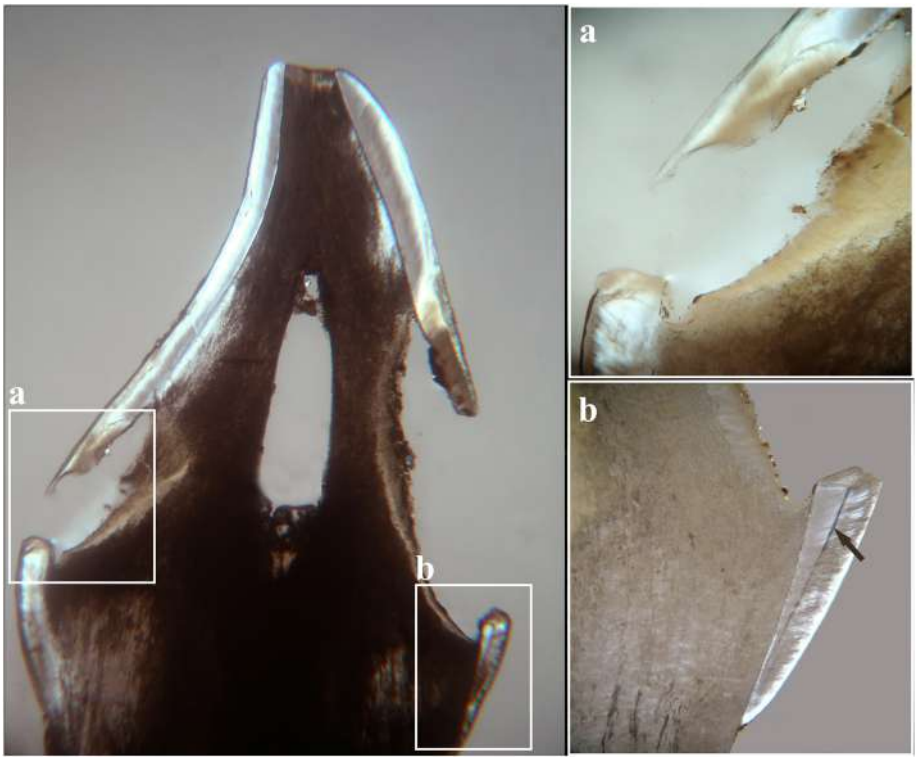

FIGURE 7 Longitudinal histological undecalcified section (10×) of one central maxillary incisor of T.43 showing the outcomes of enamel and dentin erosive lesions. The white rectangles in the section indicate the two details (20×): (a) localized brown opaque areas (positively birefringent) in the subsurface of enamel. Sclerosis of the dentin is also visible in the area of enamel breakdown. (b) The neonatal line (NL) is observable as a thick black line near the CEJ (indicated by the black arrow). [Colour figure can be viewed at wileyonlinelibrary.com]

3.3 | Mx1-SU423

At first observation, the preserved deciduous dentition was characterized by evident enamel defects, which include yellow-brownish discoloration of the crowns and marked loss of tissues.

Of the anterior dentition, only the right lateral incisor (Rdi2), which showed a defect extending from the labial to the lingual surface through the mesial side, was preserved. Most involved was the labial surface, which exhibited a large quadrangular cavity approximately in the middle of the crown, which spared the incisal and cervical regions (Figures 13a and 14a). The defect extended linearly to the mesial and lingual surfaces (Figures 13d and 14b).

The molars were all involved almost circumferentially. The defects were mainly located on the buccal and lingual surfaces, sometimes joined by the interproximal sides (Figure 13c,d). The occlusal surfaces appeared to be all affected by a marked wear of the intercuspal

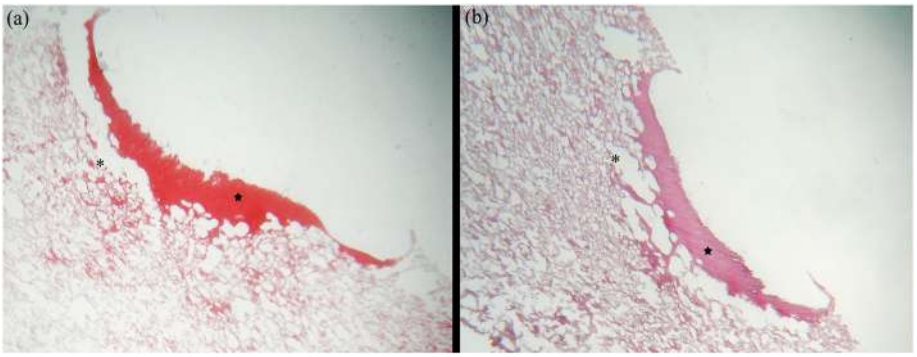

FIGURE 8 Decalcified sections of the two maxillary central incisors of T.43 stained with toluidine blue-basic fuchsin (left) and hematoxylin–eosin (right). Dentin erosion (indicated by the black asterisk) and new formation (shown by the black star), in the form of areas of tubule-rich tissue below the enamel breakdown, are evident in both sections. [Colour figure can be viewed at wileyonlinelibrary.com]

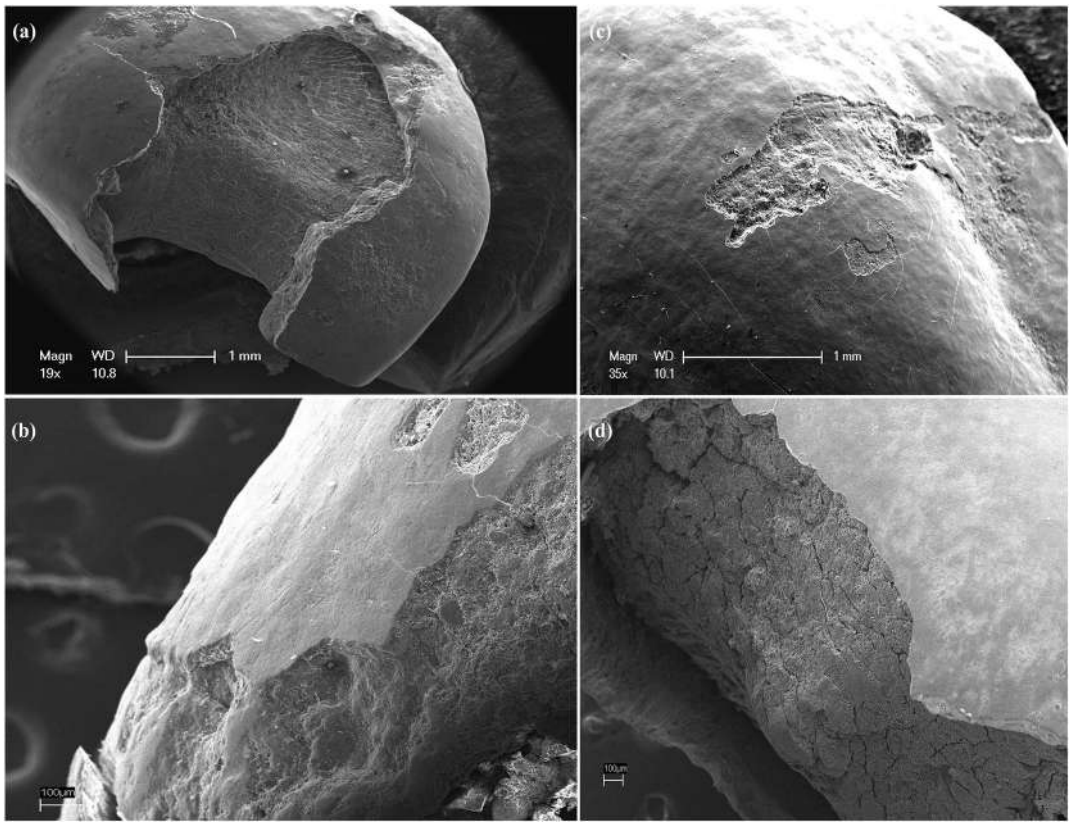

FIGURE 9 SEM images of four maxillary affected teeth of T.43. (a) Left lateral incisor showing a wide area of enamel breakdown and dentin erosion. The enamel layer uncovered by the superficial tissue loss presents a rounded edge toward the area of dentin exposure (the scale bar equals 1 mm). (b) Right canine exhibiting a localized superficial lesion of the enamel (the scale bar equals 100 µm). (c) Right first molar displaying several circular depressions in the areas of superficial enamel breakdown (the scale bar equals 1 mm). (d) Right lateral incisor presenting sharp and irregular margins of affected enamel and extensive dentin erosion (the scale bar equals 100 µm).

portion; moreover, they showed erosive lesions in the enamel and dentin tissues (Figure 13b).

Furthermore, portions of alveolar and palatal bone appeared also affected by a diffuse porosity and new deposition in the form of a thin and porous layer especially in the anterior maxillary surface, around the infraorbital foramen and surrounding the alveolar bone (Figure 13a,c), in the palatal lamina (Figure 13b,d), on the inferior surface of the orbital cavity, and in the posterior portion of the zygomatic process.

A detailed description of the observed lesions in teeth is shown in Table 5.

4 | DISCUSSION

During the analysis of the dental lesions found on the teeth of the three subjects, the presence of dentin reaction at the sites of the lesions, in the form of areas of tubules-rich tissue, was recorded. Therefore, we excluded the possibility of a postmortem nature of the lesions, although it cannot be ruled out that during the depositional period, small fractures and chippings of the thin overhanging margin of enamel may have occurred.

The three individuals described here represented a unicum within the entire anthropological record recovered in the site. In the analyzed

TABLE 3 Results of the SEM-EDS analyses performed to compare the ion content of the surface enamel at the cervical area, the yellow-brownish discolored region, and the area of enamel breakdown in one affected crown (Ldi2) of T.43, with the apparently sound enamel of a primary tooth from another individual of the same age at death.

	Control sample		Cervical enamel		Discolored enamel		Breakdown of enamel	
	Weight%	Atomic%	Weight%	Atomic%	Weight%	Atomic%	Weight%	Atomic%
Carbon	15.03	23.70	12.51	19.84	55.61	73.58	44.06	54.70
Oxygen	47.15	55.81	51.02	60.75	12.88	12.79	43.47	40.51
Phosphate	9.32	5.70	11.43	7.03	8.88	4.56	1.77	0.85
Calcium	20.82	9.84	22.77	10.82	19.90	7.89	2.97	1.11

Note: For each analyzed area, the weight percentage and the atomic percentage of the ions are reported.

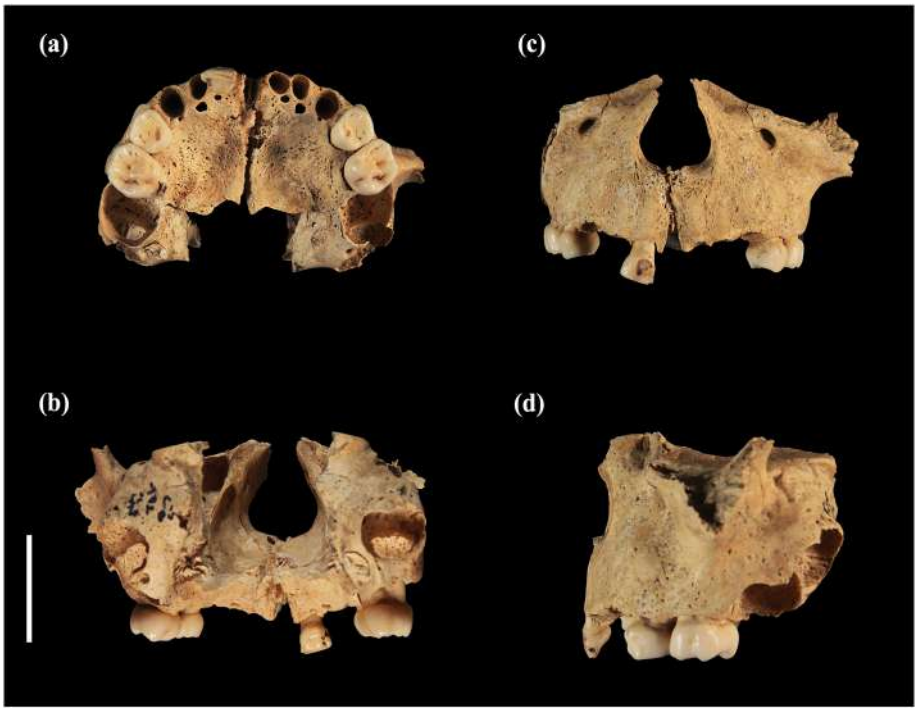

FIGURE 10 Maxillary bones and teeth of T.72. (a) Inferior (palatal) view of the maxilla showing the occlusal surface of the preserved teeth. Some small pinpoint-shaped caries in the intercuspal region of the molars and wear of the cusps, especially of the first molars, are observable. (b) Posterior view of the maxilla: Small circular erosions are visible on the lingual side of the right central incisor. (c) Anterior view of the maxilla showing extensive erosion on the lingual surface of the right central incisor. (d) Left lateral view of the maxilla displaying a circular erosion on the mesial surface of the right central incisor. Porosity, branched furrows, and bone deposition are visible on the maxillary bones. The scale bar equals 2 cm. [Colour figure can be viewed at wileyonlinelibrary.com]

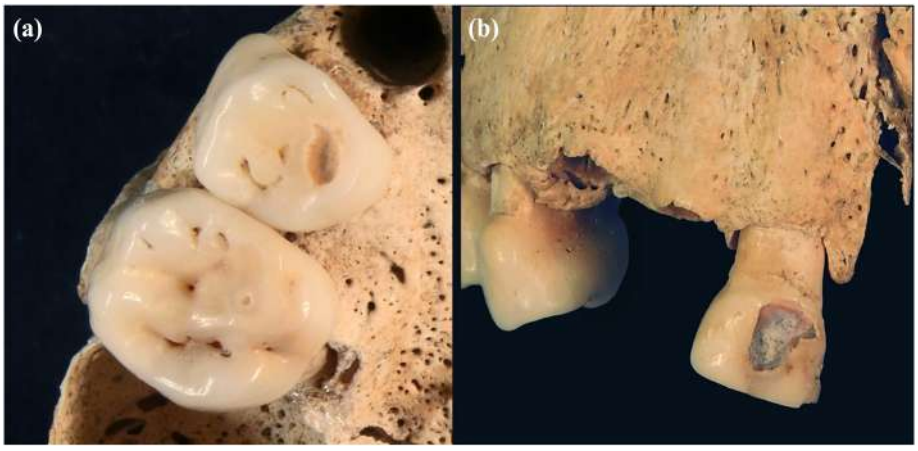

FIGURE 11 Details of some teeth of T.72. (a) Occlusal surface of Rdm2 showing small pinpoint-shaped caries in the intercuspal space. The wear of the cusps of Rdm1 is also visible. (b) Extensive lesion on the labial surface of Rdi1. [Colour figure can be viewed at wileyonlinelibrary.com]

skeletal population, we reported skeletal and dental conditions related to stress and malnutrition in subadults and women deceased in fertility window.

In the overall study, it was possible to analyze the teeth of 26 subadults (of the 52 found in the cemetery), for a total of 303 deciduous and permanent teeth. The rates calculated in the different age groups

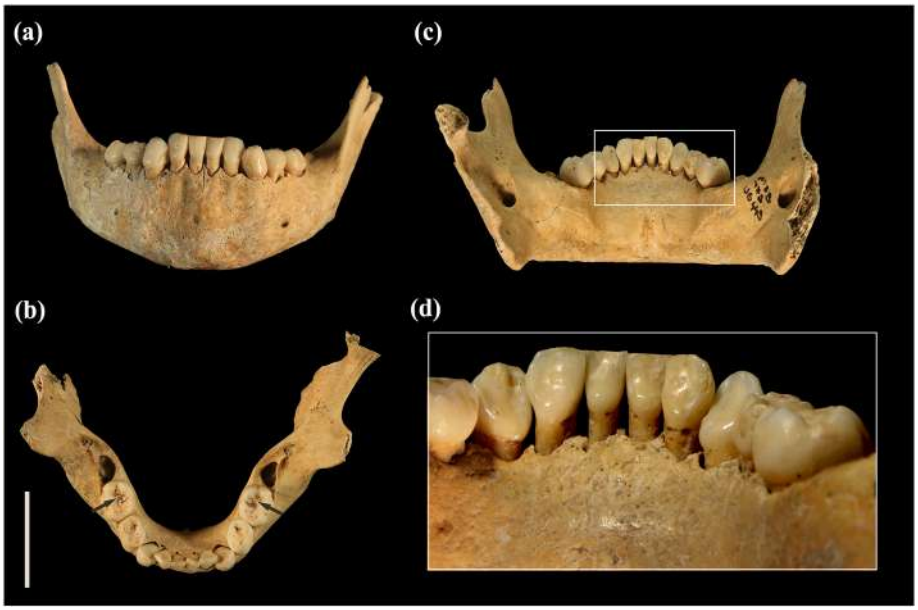

FIGURE 12 Mandibular teeth of T.72. (a) Anterior view of the mandible: Circular pitted defects and notch-like defects are visible on the labial surfaces of anterior teeth. (b) Occlusal view of mandibular teeth: Irregularities in occlusal enamel and early wear of the molars' cusps are observable (indicated by black arrows). (c) Posterior view: Circular pitted defects are visible on the lingual surface of anterior teeth; two larger areas of defective enamel are observable on the lingual side of the left canine and the right first molar. The white rectangle shows a magnified detail of the lingual side of teeth. (d) Detail of the lingual surface of teeth: Areas of defective enamel are visible on the lateral incisors in the form of pitted defects; wider defects with dentin exposure are observable on the left canine and right first molar. The scale bar equals 2 cm. [Colour figure can be viewed at wileyonlinelibrary.com]

described an infant class particularly affected by caries compared with subadults relevant to the other age categories. In fact, 57.1% of infants were affected by caries against 20% of the class of children. Moreover, evidence of hypoplastic and enamel defects was found on the deciduous and permanent teeth of the subadult individuals. Out of 26 subadults whose teeth could be examined, 65.4% had hypoplasia or evidence of enamel defects. Of the total number of teeth analyzed (Obs = 295), 34.6% are affected by defects.

The subadult class was also characterized by the presence of pathological indicators of the skeleton such as abnormal porosity, increased vascular response, and subperiosteal new bone formation related to inflammatory states and infectious and noninfectious factors (Pitre et al., 2016). Out of the total number of districts evaluated, 69.3% showed at least one of the aforementioned indicators. In particular, the deposition of subperiosteal bone in the form of a thin network of newly formed porous layer, mainly prevalent on iliac bones, diaphyses of the long bones, scapulae, and cranial tables, was detectable in 25.6% of observations. Among all the subadults, the class of infants presented the highest rates of indicators (74.5%).

As regards the category of women in the fertility range (15–45 years old), the rate of caries on the total number of teeth (37.4%) appeared to be higher than that of men of the same age interval (26%). Moreover, female subjects exhibited higher antemortem tooth loss values than male individuals in almost all localizations. The frequencies of hypoplasia in females were equal to 36.4% of the total number of teeth examined, with rates of hypoplasia on the posterior teeth higher than those of the opposite sex. Evidence of periostitis was detected in the active and repaired form in 7.7% of the total bone portions considered, in particular in the alveolar bone (19%) and in the lower limbs (13.3%). Stress indicators, in the form of *cribra cranii* and *cribra orbitalia*, showed a total rate of 65.6%, with a prevalence of *cribra orbitalia* (83.3%) over *cribra cranii* (61.5%) in the female sample. In general, the detection of slight porosity was prevalent (53.1%) compared with that of medium–strong degree (12.5%). However, *cribra orbitalia* were present in higher rates in the moderate–strong degree than in the mild one (66.7% and 16.7%).

Some pathological indicators of stress and malnutrition were detected in the females and infants of the sample, allowing us to formulate hypotheses of deficiencies and nutritional issues at the origin of chronic metabolic and hematological disorders. The hematological evidence is the result of megaloblastic anemia acquired by infants through the maternal deficiency of vitamin B12 that favors further nutrient losses through gastrointestinal infections during the period of weaning (Walker et al., 2009).

The three cases treated here showed intense alterations to the enamel of the deciduous dentition, suggesting congenital or acquired disease. In the most serious cases, lesions involve the entire crown circumferentially up to its almost total destruction (Figure 4a). In order to perform a thorough differential diagnosis, dental fluorosis (DF), molar incisor hypomineralization (MIH), congenital syphilis (CS), amelogenesis imperfecta (AI), plane-form enamel hypoplasia (PFEH) with nonspecific cause, DDE, and ECC were taken into considerations.

Fluorosis is a metabolic disturbance caused by an excessive assumption of fluorine, leading to defects to both the skeleton and

TABLE 4 Detailed description of the dental lesions observed on T.72.

Tooth	Side	Surfaces	Defect type	Description
Maxilla				
di1	R	Labial, lingual, mesial, distal	Enamel loss, dentin erosion, enamel discoloration	Wide labial cavity, oval-shaped, located between the incisal third and the cervical third of the crown, occupying almost its entire length. On the lingual side, a coalesced defect along the distal margin continues seamlessly in the interproximal distal surface, affecting almost the entire length of the crown. On the mesial side, a small pointed defect is observed near the incisal tip. Deep dentin erosion is visible beneath the enamel loss.
dm1	R	Occlusal	Wear	Flattening and marked wear of the occlusal cusps with exposure of dentin are detected.
	L	Occlusal	Wear, enamel erosion	Flattening and marked wear of the occlusal cusps with exposure of dentin are detected. A pinhole defect is observed on the occlusal surface.
dm2	R	Occlusal	Enamel erosion	Points of enamel erosion in the form of pinhole defects are recorded between the occlusal cusps.
	L	Occlusal	Enamel erosion	Points of enamel erosion in the form of pinhole defects are recorded between the occlusal cusps.
Mandible				
di1	R	Labial	Enamel defects	Circular pitted defects of enamel are visible on the labial surface.
	L	Labial	Enamel defects	Circular pitted defects of enamel are visible on the labial surface.
di2	R	Labial, lingual	Dentin erosion, enamel defects	Small and superficial areas of erosion of the root tissues along the cervical border are noted on the lingual side. Circular defective areas of enamel are present on the lingual and labial surfaces.
	L	Labial, lingual	Enamel defects	Circular defective areas of enamel are visible on the lingual and labial surfaces.
dc	R	Labial, mesial, distal	Enamel defects	Areas of enamel defects are observed on the labial and interproximal surfaces.
	L	Lingual, mesial	Enamel defects	A defective oval area with dentin exposure is visible on the lingual surface near the occlusal edge. A pinpoint defect of enamel is present on the mesial surface.
dm1	R	Buccal, lingual, mesial	Enamel defects, discoloration	A small circular defect is located on the mesial surface, occupying the middle third of the crown length, with exposure of the dentin. A notch-like defect is visible on the mesiobuccal side. On the lingual side, a wide area of defect with dentin exposure is observed in the middle third of the crown. Discoloration of the crown with opaque white patches is present in the occlusal third of the crown. Irregularities in occlusal enamel deposition, with early wear of the cusps, are observed.
	L		Enamel defects	Circular pitted defects of enamel are visible on the buccal surface. Irregularities in occlusal enamel deposition are observed, with early wear of the cusps.
dm2	R		Enamel defects, discoloration	Discoloration of the crown presenting opaque white patches is detected in the occlusal third of the crown. Irregularities in occlusal enamel deposition are observed, with early wear of the cusps.
	L		Enamel defects, discoloration	Discoloration of the crown presenting opaque white patches is detected in the occlusal third of the crown. Irregularities in occlusal enamel deposition are observed, with early wear of the cusps.

Note: For each affected tooth, the side, surfaces, and type of defect are indicated.

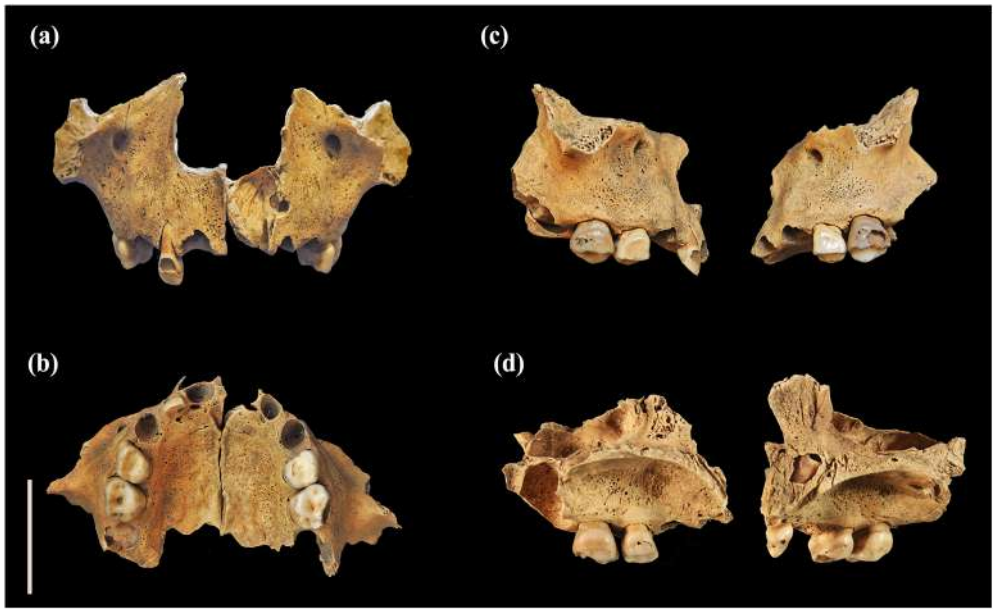

FIGURE 13 Maxillary bones and teeth of Mx1-SU423. (a) Anterior view of the maxilla showing extensive erosion on the labial surface of the right lateral incisor. (b) Inferior (palatal) view of the maxilla showing the occlusal surface of the preserved teeth. Some cavitations affecting the occlusal surface of the molars and early wear of the cusps are observable. (c) Lateral view of the maxillary bones displaying extensive erosions on the buccal surfaces of the molars. (d) Medial view of the maxillary bones displaying linear erosions on the lingual surfaces of molars and on the lingual and mesial surfaces of the right lateral incisor. Porosity, branched furrows, and bone deposition are visible on the maxillary bones. The scale bar equals 2 cm. [Colour figure can be viewed at wileyonlinelibrary.com]

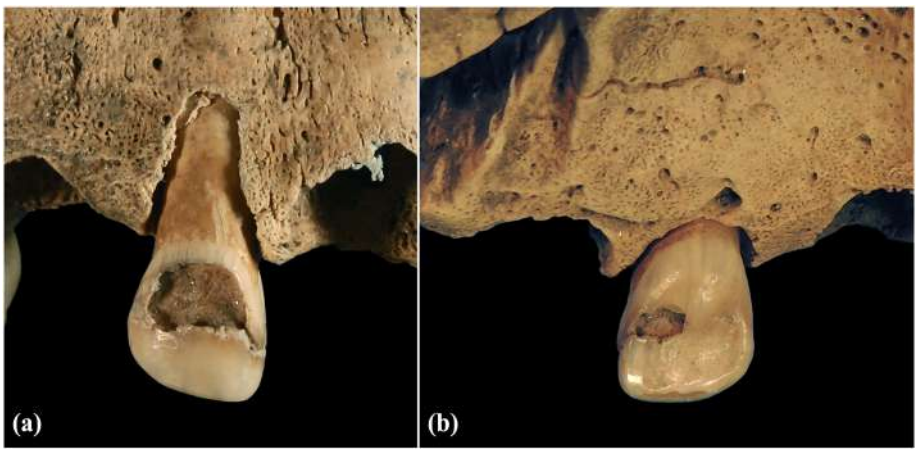

FIGURE 14 Details of the right lateral incisor of Mx1-SU423. (a) Extensive quadrangular lesion on the labial surface of Rdi2. (b) Lesion on the lingual surface of Rdi2, in continuity with the labial lesion through a linear erosion on the mesial side. [Colour figure can be viewed at wileyonlinelibrary.com]

teeth. An excess of fluorine may provoke mottling of enamel (Nelson et al., 2019). DF, characterized by fine white lines to chalky and brittle enamel or pitting, reflects disturbances during the phase of enamel formation (Blau et al., 2002). Although our findings of pitted and discolored enamel, in particular on the mandibular dentition of T.43 and T.72, could present similarities with the alteration of DF, some studies showed that changes are mostly expressed on the later developing teeth, especially the second molars, as DF is associated with postnatal fluoride level (Warren et al., 2001). In our cases, the anterior deciduous dentition appeared to be the most affected together with the molars, rather suggesting a prenatal and perinatal involvement. These characteristics allow us to rule out this diagnosis.

MIH is a condition found especially in first permanent molars and incisors. It is due to systemic disturbances to ameloblast function occurring during the mineralization phase and resulting in defective enamel with an increased protein content (Subramaniam et al., 2016). Hypomineralized enamel varies from opacity or discoloration to areas of enamel breakdown with exposition of dentin and caries development (Weerheijm et al., 2001). MIH-like defects are also described to affect the deciduous dentition, in particular second primary molars (Elfrink et al., 2012). This condition is known as deciduous molar hypomineralization (DMH). These enamel alterations are similar to those observed in our samples. However, in our case, the dentitions are more widely

TABLE 5 Detailed description of the dental lesions observed on Mx1-SU423.

Maxilla				
Tooth	**Side**	**Surfaces**	**Defect type**	**Description**
di2	R	Labial, lingual, mesial	Discoloration, enamel loss, dentin erosion	Wide labial area of enamel loss, quadrangular in shape, located between the central third and the cervical third of the crown. On the lingual side, the defect continues seamlessly through the interproximal mesial surface, affecting only the mesial half of the surface, at the middle of the crown. Dentin erosion is visible beneath the enamel loss. Brownish discoloration involves almost the entire crown, sparing a thin cervical band.
dm1	R		Discoloration, enamel loss	Superficial and linear areas of defects are present in the mesial and lingual surfaces, forming a continuous and subtle lesion. Discoloration involves the occlusal and central thirds of the crown and almost the entire buccal surface. Linear white opacities are observed along the discoloration borders.
	L		Discoloration, enamel loss	The defects are localized on the lingual, mesial, and occlusal surfaces in the form of linear lesions. On the lingual surface, the enamel appears eroded and small cavitation in the tissue is identified. The defect continues together with the mesial one. On the occlusal surface, the linear lesion involves the lingual cusps. Discoloration affects the occlusal and central thirds of the crown.
dm2	R		Discoloration, enamel loss, dentin erosion	The defects are located on the buccal, lingual, and occlusal surfaces. The buccal surface shows a large lesion and small cavitation is also visible inside the area. Four cavitations affect the occlusal surface, two smalls on the distal cusp, one very small on the mesial side, and one more extensive and deeper in the intercuspal region. Discoloration involves the occlusal and central thirds of the crowns. Linear white opacities are observed along the discoloration borders.
	L		Discoloration, enamel loss, dentin erosion	The defects are located on the buccal, lingual, and occlusal surfaces. The buccal surface shows an extensive lesion in the form of large cavitation involving almost the entire surface and a second area of more superficial defect, interested by a small cavity. Two cavitations affect the occlusal surface, on the distal cusp and the intercuspal region. Discoloration involves the occlusal and central thirds of the crown. Linear white opacities are observed along the discoloration borders.

Note: For each affected tooth, the side, surfaces, and type of defect are indicated.

affected, not allowing the evidence to be diagnosed as DMH alone.

CS affects tooth and enamel formation, causing specific dental signs that are diagnostic of the disease, such as Hutchinson's incisors, Moon molars, and mulberry molars, together with a spectrum of variations including notches, severe hypoplasia and hypoplastic nodules, grooves, and pits (Ioannou et al., 2018). As our cases lack specific diagnostic features, we can exclude this diagnosis at the origin of the evidence found.

AI represents a group of conditions, genomic in origin, which affect the structure and clinical appearance of the enamel of all or nearly all the teeth in an equal manner. It is caused by mutations in the genes controlling amelogenesis and follows patterns of autosomal dominant, autosomal recessive, or X-linked inheritance. Amelogenesis is disturbed in a precise moment of its activity, resulting in different enamel defects (Wasterlain & Dias, 2009). In our specimens, not all the teeth are affected, displaying different patterns of expression. Moreover, in AI, the enamel shows reduced radiodensity in relation to dentin, a feature that is not present in our case. For these reasons, we can rule out the diagnosis of AI.

DDE are defects associated with systemic insults that disrupt the cellular activity of ameloblasts during tooth formation. The type of defect depends on the moment of the stress onset and therefore the disturbance to ameloblastic activity. These imperfections of the crown are discernible as areas of defective or thinned enamel in the form of linear, oval, or roughly circular areas, or of flattened or concave pits (Halcrow & Tayles, 2008). Pit-form defects are due to failure of clusters of ameloblasts that stop forming enamel matrix, resulting in isolated small or large pits, rows of pits, or in a broader band around the circumference of the crown (Hillson & Bond, 1997). Plane-form

defects are the outcome of the plane of a brown stria of Retzius left exposed by the ceasing of enamel matrix; several planes of brown striae can be involved, giving the defect a stepped appearance with the normal surrounding enamel (Hillson & Bond, 1997).

The current definition of ECC (American Academy on Pediatric Dentistry & American Academy of Pediatrics, 2016) cites one or more evidence of decayed, missing, or filled tooth (DMFT) anywhere in the primary dentition of children under the age of six. As regards S-ECC, the definition requires the presence of any instance of smooth surface affected by caries in pediatric age, especially under the age of three, missing or filled tooth in the deciduous maxillary anterior teeth. S-ECC causes rapid and extensive demineralization of dental tissues that at the outset establishes as an area of opacity of the enamel and then progresses to discoloration and to the final enamel and dentin destruction. In most advanced cases, crowns can be completely destroyed by the widespread of the decaying process (Ripa, 1988). Ripa (1988) reported that maxillary anterior teeth are the most affected by the rampart caries, whereas mandibular teeth are usually spared. The other teeth can be involved depending on the duration of the carious process, but the lesions are less severe than those of the maxillary incisors.

In our cases, maxillary dentition is affected by the most severe changes, which involve lesions to the enamel ranging from small areas to large, scooped defects and extensive circumferential bands, erosion of the underlying dentin up to the total destruction of the crown (Figures 4a, 10, and 13). The mandibular teeth, on the other hand, show small defects with the formation of areas, grooves, or pits of missing or thinned enamel, without however presenting extensive destruction of the hard dental tissues (Figures 4b and 12).

The changes observed in the primary crowns of T.43, T.72, and Mx1-SU423, characterized by areas of enamel destruction and of deep dentin erosion, are consistent with severe early carious decaying (S-ECC). The aggressiveness of caries and their speed of progression, given the few years of life of those children, and the preference for surfaces usually not attacked by caries (Moore & Corbett, 1973) suggested that these have developed on a tissue previously weakened. Moreover, the superficial defects, in the form of pits and circular areas of enamel loss, conform to the pitted and plane-form EH types described by Hillson and Bond (1997) and Hillson (2001). Furthermore, several teeth showed yellow-brownish pigmentation of the crown, suggesting hypomineralized hard tissues. These defects are consistent with disturbances that occurred during the enamel formation. In fact, disruption during the secretion phase of ameloblasts can lead to quantitative defects and hypoplastic changes, and disturbances during the maturation stage induce hypomineralization regardless of the formation of hypoplasia (Suga, 1989). The presence of previous defective enamel structure is one of the most predisposing causes to caries (Halcrow & Tayles, 2008).

The occurrence of circular caries, though, tends to hide previous defects (Oliveira et al., 2006), as they destroy the enamel and corrode underlying dentin, masking any preexisting evidence. In fact, caries in primary dentition normally take 1 year to breach the outer layer of enamel and 3 years to reach the dentin (Schuurs, 2013). Furthermore, it has been recorded in literature that smooth surfaces such as the buccal and lingual ones take much longer to reach an advanced stage (Schuurs, 2013), thus causing the S-ECC type. Some children can develop this aggressive type of decay on any smooth surfaces before 36 months after birth. Therefore, in young infants and children, it is possible to suggest that something no longer visible has conveyed the rapid formation of caries. In particular, a linear position of caries progressing toward the occlusal tip, from incisors to molars, seems to track an underlying alteration that occurred in a single time range and then the formation of defects in different levels of crowns, depending on the timing of tooth development (Caufield et al., 2012; referring to as the typical "frown" pattern).

Histological sections performed on the teeth of T.43 showed isolated brown opaque areas as positively birefringent lesions in the subsurface of enamel near the areas of breakdown, revealing caries progression underneath the external surface, and advanced dentin sclerosis (Figure 7a) (Gupta et al., 2020); moreover, tertiary dentin was identified in form of a tubules-rich tissue in the areas of lesion (Figure 8). SEM images further showed the outcomes of the decaying process affecting the hard tissues; moreover, in the areas of superficial enamel breakdown, several circular depressions of the surface are visible (Figure 9b), possibly connected to preexisting enamel defects.

Furthermore, SEM-EDS analyses (Table 3) allowed us to consider the mineral composition of the adamantine surfaces of one affected tooth from T.43. The exam revealed that the intact cervical enamel zone on the tooth with defects had comparable Ca and P content as the control. The enamel zone presenting discoloration had slightly lower Ca and P content, much higher amount of C, and lower O. The area of enamel breakdown presented much higher C with lower O content and much lower amount of Ca and P than the control tooth. These analyses suggested the existence of enamel hypomineralization in the discolored and damaged enamel, cervical enamel appeared sound and comparable with the control tooth. The recorded increase in the C content of the affected tooth may indicate the retention of organic substance, probably because of defects in the enamel maturation (Bozal et al., 2015).

The analysis of the investigated individuals also suggested the existence of a possible metabolic condition, indicated by the presence of islands of porous subperiosteal new bone, fine, abnormal cortical porosity, and vascular impressions (Snoddy et al., 2018). According to the literature, these features found in several diagnostic anatomical locations may be consistent with generalized physiological conditions, rather than with localized inflammatory phenomena, and in particular with metabolic and deficiency disorders (Klaus, 2014; Snoddy et al., 2018). Such evidence of diffuse hyperplasia and abnormal porosity on the skeleton have been correlated with chronic episodes of abnormal bleeding and connected with an evaluation of scurvy (Snoddy et al., 2018). This finding allowed us to assume a possible correlation between the osseous lesions and the dental condition, both associated with deficiencies and nutritional issues.

The carious lesions observed are thereby consistent with preexisting DDE, to which probably extrinsic factors occurred after the eruption in the oral environment superimposed the development of

particularly rapid and aggressive decaying. The relatively linear course of the lesions, which degrades toward the occlusal surface moving from anterior to posterior teeth (Figures 4a and 13), suggested the presence of underlying defects of enamel that occurred during a specific period of crown formation. In accordance with the dental mineralization tables, the lesions detected seemed consistent with defects arisen in the fetal period and protracted in the early months after birth. The development in the fetal period could be hypothesized based on the position of the lesions in the crown (Table 1) and the extension of the discoloration area that in most cases involved the entire crown up to a few millimeters from the CEJ (Figures 4a and 5). According to the literature, the crown of the first maxillary incisor at birth is formed at 60%–80% (Hillson, 2009) and has a length of about 5 mm (Irurita et al., 2014; Minier et al., 2014). According to these estimates, in all three specimens, the lesions on the maxillary central incisors appeared to be related to defects arising in the prenatal-forming enamel. On the other hand, the defects affecting the canines that were localized on the midlabial surface attested to disorders occurring in the postnatal period, because only the cuspal 1/3 of the tooth is formed during gestation (Halcrow & Tayles, 2008). The lesions affecting the molars, located both on the occlusal surface and on the lateral ones, confirmed disturbances that occurred in the perinatal and postnatal period because the crown at birth is formed only at the stage of completion of the occlusal surface. In addition, the longitudinal section of the maxillary incisor of T.43 clearly showed the neonatal line (Figure 7b) that was located externally with respect to the position of the subsurface defect, indicating that the enamel toward the dentin-enamel junction was the one deposited before birth and the external and cervical one was postnatal compared with the line.

Enamel defects on deciduous dentition are significant, as they can manifest during the fetal development, suggesting the poor health conditions of the mother (Cook & Buikstra, 1979; Ghapanchi et al., 2015). Recently, clinical literature has increasingly focused on the prevalence and etiology of DDE in the primary dentition of preschool children, as indicators of general health during infancy. Actual prevalence of DDE in primary dentition ranges in different populations worldwide between 8.5% and 48% (Carvalho et al., 2011; Massignan et al., 2016).

Studies on contemporary populations have revealed that several factors are correlated to the development of defects in enamel, including prenatal, perinatal, and postnatal issues and local, systemic, genetic, or environmental conditions. Identified causes range from maternal to various child factors, such as preterm birth; low birthweight; traumatic delivery; pregnancy-related complications such as infections, illness, parasitic infestations, metabolic diseases, deficiencies, uterine, and placental abnormalities; and other gestational issues (Caufield et al., 2012; Ghapanchi et al., 2015; Jacobsen et al., 2013; Norén, 1984; Oliveira et al., 2006; Reed et al., 2017; Seow, 2014). Further, maternal-related fetal malnutrition and nourishing deprivation of the newborn appear in several studies to be linked to enamel hypoplasia and defects on deciduous dentition (Enwonwu, 1973; Oliveira et al., 2006). Influence of socioeconomic conditions on dental defects has been proven by cross-sectional and cohort studies on children from underdeveloped areas (Enwonwu, 1973), or among those living at or below poverty (Caufield et al., 2012; Oliveira et al., 2006).

Based on the frequent association between DDE and caries, Caufield et al. (2012) proposed the new classification of defects-related decay as hypoplasia-associated severe early childhood caries (HAS-ECC). This type of caries affects mostly infants living in the condition of poverty (American Academy on Pediatric Dentistry & American Academy of Pediatrics, 2016; Oliveira et al., 2006) or characterized by an antecedent common condition such as prematurity or low birthweight (Velló et al., 2010).

For what concern posteruptive factors, nutritional aspects must be considered in childhood caries, especially those administered during weaning or as a substitute for breastfeeding. S-ECC are also known as "nursing bottle caries" or "baby bottle caries," especially when primary maxillary incisors are extensively affected, because drink is suckled and conveyed to the upper anterior teeth (Cook & Buikstra, 1979). Composition, frequency of intake of the diet, and specific behaviors can play a role in the caries progression, together with the presence of cariogenic bacteria and oral pathogens. Emergence in the mouth exposes defective teeth to the colonization by bacteria and to the attack of enamel by sugars and acids of diet, accelerating the caries process (Caufield et al., 2012).

Association between iron-deficiency anemia and S-ECC in modern patients (Clarke et al., 2006) finds its counterpart in osteoarchaeological studies, where a positive correlation has been found between the presence of *cribra orbitalia* and caries in children (O'Sullivan et al., 1992), demonstrating the role that nutritional stresses have in early caries etiology (Alaluusua, 2012).

The detection of circular caries on the primary dentition is an indicator of stress in osteoarchaeological samples that informs us about health conditions, social status, feeding practices, and access to nutritional resources (Cook & Buikstra, 1979).

Furthermore, the detection of enamel defects associated with severe early caries in subadults allows us to relate these findings with the age-at-death and investigate whether a correlation exists between weaning age mortality and the presence of DDE (Cook & Buikstra, 1979). This aspect is particularly interesting as it opens a window on infant nutrition and risk of death and on selection against impaired individuals in specific moments marked by food changes, nutritional stresses, or diseases.

5 | LIMITATIONS OF THE STUDY

Dealing with osteoarchaeological populations, it is not possible to establish the prevalence and incidence of this condition, being the analyses based on mortality samples. If we consider infant caries as a disorder associated with other conditions, previously arisen, or acting synergistically, the possibility that the selected children could have had more severe caries than the surviving members of the community should be taken into account (O'Sullivan et al., 1992).

In this case, the tracing of these alterations in three individuals belonging to different periods, together with the limitation given by the small sample size, does not allow us to deduce any data on the prevalence of this type of pathological changes in the ancient population.

6 | CONCLUSIONS

In the cases analyzed, the defects appeared to have arisen during the fetal period and then protracted in the postnatal life. In both cases, it is possible to suggest that they are related to in utero health.

The observation of indicators of metabolic diseases as a probable scurvy affection in the three individuals supports the suggestion that the pathological evidence is correlated to a systemic picture of stress and nutritional deficiency. According to several authors, DDE could have exposed children to premature death in a crucial moment of life, such as during the transition from breastfeeding to weaning (Cook & Buikstra, 1979).

Based on these findings and the premature selection of these children, it is possible to hypothesize that secondary issues, such as oral infections, nutritional impairment, and systemic disturbances, had occurred complicating an already complex health picture and challenging these infants' chances of survivorship.

ACKNOWLEDGMENTS

We would like to thank the Superintendence of Archaeological Heritage of Lombardy for the direction of the archaeological investigations at the site of San Biagio in Cittiglio. In addition, we thank Regione Lombardia, Fondazione Cariplo, and Fondazione Comunitaria del Varesotto for their financial support to archaeological and anthropological analyses. Thanks also go to the Unitech Office (University Technology Platforms of the University "Statale" of Milan) for having conducted the SEM analyses on some teeth of the samples.

CONFLICTS OF INTEREST STATEMENT

The authors declare no conflict of interest.

DATA AVAILABILITY STATEMENT

The data that support the findings of this study are available from the corresponding author upon reasonable request.

ORCID

Roberta Fusco https://orcid.org/0000-0001-5443-8364
Marta Licata https://orcid.org/0000-0003-3343-3999

REFERENCES

Alaluusua, S. (2012). Defining developmental enamel defect-associated childhood caries: where are we now? *Journal of Dental Research*, *91*(6), 525–527. https://doi.org/10.1177/0022034512445634

AlQahtani, S. J., Hector, M. P., & Liversidge, H. M. (2010). Brief communication: the London atlas of human tooth development and eruption. *American Journal of Physical Anthropology*, *142*(3), 481–490. https://doi.org/10.1002/ajpa.21258

American Academy on Pediatric Dentistry & American Academy of Pediatrics (2016). Policy on early childhood caries (ECC): classifications, consequences, and preventive strategies. *Pediatric Dentistry*, *38*(6), 52–54.

Aminabadi, N. A., Oskouei, S. G., Pouralibaba, F., Jamali, Z., & Pakdel, F. (2009). Enamel defects of human primary dentition as virtual memory of early developmental events. *Journal of Dental Research, Dental Clinics, Dental Prospects*, *3*(4), 7.

Blau, S., Kennedy, B. J., & Kim, J. Y. (2002). An investigation of possible fluorosis in human dentition using synchrotron radiation. *Journal of Archaeological Science*, *29*(8), 811–817. https://doi.org/10.1006/jasc.2001.0657

Bonsall, L., Ogden, A. R., & Mays, S. (2016). A case of early childhood caries from Late Roman Ancaster, England: a case of early childhood caries from Roman Britain. *International Journal of Osteoarchaeology*, *26*(3), 555–560. https://doi.org/10.1002/oa.2441

Bozal, C. B., Kaplan, A., Ortolani, A., Cortese, S. G., & Biondi, A. M. (2015). Ultrastructure of the surface of dental enamel with molar incisor hypomineralization (MIH) with and without acid etching. *Acta Odontológica Latinoamericana*, *28*(2), 192–198. https://doi.org/10.1590/S1852-48342015000200016

Cardoso, H. F. V., Meyers, J., & Liversidge, H. M. (2019). A reappraisal of developing deciduous tooth length as an estimate of age in human immature skeletal remains. *Journal of Forensic Sciences*, *64*(2), 385–392. https://doi.org/10.1111/1556-4029.13892

Carvalho, J. C., Silva, E. F., Gomes, R. R., Fonseca, J. A. C., & Mestrinho, H. D. (2011). Impact of enamel defects on early caries development in preschool children. *Caries Research*, *45*(4), 353–360. https://doi.org/10.1159/000329388

Castro, M. J., Mendes, J. J., Vinga, S., & de Andrade, D. C. (2021). Differential diagnosis of developmental defects of enamel: a review. *Annals of Medicine*, *53*(sup1), S37. https://doi.org/10.1080/07853890.2021.1897305

Caufield, P. W., Li, Y., & Bromage, T. G. (2012). Hypoplasia-associated severe early childhood caries—a proposed definition. *Journal of Dental Research*, *91*(6), 544–550. https://doi.org/10.1177/0022034512444929

Clarke, M., Locker, D., Berall, G., Pencharz, P., Kenny, D. J., & Judd, P. (2006). Malnourishment in a population of young children with severe early childhood caries. *Pediatric Dentistry*, *7*.

Clarkson, J., & O'Mullane, D. (1989). A modified DDE index for use in epidemiological studies of enamel defects. *Journal of Dental Research*, *68*(3), 445–450. https://doi.org/10.1177/00220345890680030201

Conceição, E. L. N., & Cardoso, H. F. V. (2011). Environmental effects on skeletal versus dental development II: further testing of a basic assumption in human osteological research. *American Journal of Physical Anthropology*, *144*(3), 463–470. https://doi.org/10.1002/ajpa.21433

Cook, D. C., & Buikstra, J. E. (1979). Health and differential survival in prehistoric populations: prenatal dental defects. *American Journal of Physical Anthropology*, *51*(4), 649–664. https://doi.org/10.1002/ajpa.1330510415

Elamin, F., & Liversidge, H. M. (2013). Malnutrition has no effect on the timing of human tooth formation. *PLoS ONE*, *8*(8), e72274. https://doi.org/10.1371/journal.pone.0072274

Elfrink, M. E. C., ten Cate, J. M., Jaddoe, V. W. V., Hofman, A., Moll, H. A., & Veerkamp, J. S. J. (2012). Deciduous molar hypomineralization and molar incisor hypomineralization. *Journal of Dental Research*, *91*(6), 551–555. https://doi.org/10.1177/0022034512440450

Enwonwu, C. O. (1973). Influence of socio-economic conditions on dental development in nigerian children. *Archives of Oral Biology*, *18*(1), 95-107, IN15. https://doi.org/10.1016/0003-9969(73)90024-1

Fédération Dentaire Internationale (FDI). (1992). Commission on oral health, research and epidemiology. A review of the developmental defects of enamel index (DDE index). *International Dental Journal*, *42*(6), 411–426.

Ghapanchi, J., Kamali, F., Siavash, Z., Ebrahimi, H., Pourshahidi, S., & Ranjbar, Z. (2015). The relationship between gestational diabetes, enamel hypoplasia and DMFT in children: a clinical study in southern Iran. *British Journal of Medicine and Medical Research*, *10*(9), 1–6. https://doi.org/10.9734/BJMMR/2015/19574

Gupta, S., Mahajan, M., Khanna, I., Yousuf, A., Gupta, A., Pabla, G. S., & Jakhar, D. (2020). Dental caries. *IOSR Journal of Dental and Medical Sciences*, *19*(8), 1–8.

Halcrow, S. E., & Tayles, N. (2008). Stress near the start of life? Localised enamel hypoplasia of the primary canine in late prehistoric mainland Southeast Asia. *Journal of Archaeological Science*, *35*(8), 2215–2222. https://doi.org/10.1016/j.jas.2008.02.002

Hillson, S. (2001). Recording dental caries in archaeological human remains. *International Journal of Osteoarchaeology*, *11*(4), 249–289. https://doi.org/10.1002/oa.538

Hillson, S. (2009). The world's largest infant cemetery and its potential for studying growth and development. *Hesperia Supplements*, *43*, 137–154.

Hillson, S. (2014). *Tooth Development in Human Evolution and Bioarchaeology*. Cambridge University Press. https://doi.org/10.1017/CBO9780511894916

Hillson, S., & Bond, S. (1997). Relationship of enamel hypoplasia to the pattern of tooth crown growth: a discussion. *American Journal of Physical Anthropology*, *104*(1), 89–103. https://doi.org/10.1002/(SICI)1096-8644(199709)104:1<89:AID-AJPA6>3.0.CO;2-8

Ioannou, S., Henneberg, R. J., & Henneberg, M. (2018). Presence of dental signs of congenital syphilis in pre-modern specimens. *Archives of Oral Biology*, *85*, 192–200. https://doi.org/10.1016/j.archoralbio.2017.10.017

Irurita Olivares, J., Alemán Aguilera, I., Viciano Badal, J., De Luca, S., & Botella López, M. C. (2013). Evaluation of the maximum length of deciduous teeth for estimation of the age of infants and young children: proposal of new regression formulas. *International Journal of Legal Medicine*, *128*(2), 345–352. https://doi.org/10.1007/s00414-013-0903-y

Jacobsen, P. E., Henriksen, T. B., Haubek, D., & Østergaard, J. R. (2013). Developmental enamel defects in children prenatally exposed to antiepileptic drugs. *PLoS ONE*, *8*(3), e58213. https://doi.org/10.1371/journal.pone.0058213

Klaus, H. D. (2014). Subadult scurvy in Andean South America: Evidence of vitamin C deficiency in the late pre-Hispanic and Colonial Lambayeque Valley, Peru. *International Journal of Paleopathology*, *5*, 34–45. https://doi.org/10.1016/j.ijpp.2013.09.002

Lacruz, R. S., Habelitz, S., Wright, J. T., & Paine, M. L. (2017). Dental enamel formation and implications for oral health and disease. *Physiological Reviews*, *97*(3), 939–993. https://doi.org/10.1152/physrev.00030.2016

Lang, J., Birkenbeil, S., Bock, S., Heinrich-Weltzien, R., & Kromeyer-Hauschild, K. (2016). Dental enamel defects in German medieval and early-modern-age populations. *Anthropologischer Anzeiger*, *73*(4), 343–354. https://doi.org/10.1127/anthranz/2016/0617

Levine, R. S., Turner, E. P., & Dobbing, J. (1979). Deciduous teeth contain histories of developmental disturbances. *Early Human Development*, *3*(2), 211–220. https://doi.org/10.1016/0378-3782(79)90009-4

Lewis, M. (2017). *Paleopathology of Children: Identification of Pathological Conditions in the Human Skeletal Remains of Non-adults*. Academic Press.

Lewis, M. E. (2013). Children of the Golden Minster: St. Oswald's priory and the impact of industrialisation on child health. *Journal of Anthropology*, *2013*, 1–11. https://doi.org/10.1155/2013/959472

Licata, M., Iorio, S., Rossetti, C., & Badino, P. (2019). The medieval church of San Biagio in Cittiglio (Varese, Northern Italy). Archaeological and anthropological investigations of the cemeterial area. *Studia Antiqua et Archaeologica*, *25*(1), 163–183.

Liversidge, H. M., Dean, M. C., & Molleson, T. I. (1993). Increasing human tooth length between birth and 5.4 years. *American Journal of Physical Anthropology*, *90*(3), 307–313. https://doi.org/10.1002/ajpa.1330900305

Liversidge, H. M., Herdeg, B., & Rösing, F. W. (1998). Dental age estimation of non-adults. A review of methods and principles. In K. W. Alt, F. W. Rösing, & M. Teschler-Nicola (Eds.). *Dental Anthropology* (pp. 419–442). Springer Vienna. https://doi.org/10.1007/978-3-7091-7496-8_21

Lunt, R. C., & Law, D. B. (1974). A review of the chronology of calcification of deciduous teeth. *The Journal of the American Dental Association*, *89*(3), 599–606. https://doi.org/10.14219/jada.archive.1974.0446

Madhusudhan, K. S., & Khargekar, N. (2020). Nutritional status and its relationship with dental caries among 3–6-year-old Anganwadi children. *International Journal of Clinical Pediatric Dentistry*, *13*(1), 6–10. https://doi.org/10.5005/jp-journals-10005-1706

Massignan, C., Ximenes, M., da Silva Pereira, C., Dias, L., Bolan, M., & Cardoso, M. (2016). Prevalence of enamel defects and association with dental caries in preschool children. *European Archives of Paediatric Dentistry*, *17*(6), 461–466. https://doi.org/10.1007/s40368-016-0254-8

Minier, M., Maret, D., Dedouit, F., Vergnault, M., Mokrane, F.-Z., Rousseau, H., Adalian, P., Telmon, N., & Rougé, D. (2014). Fetal age estimation using MSCT scans of deciduous tooth germs. *International Journal of Legal Medicine*, *128*(1), 177–182. https://doi.org/10.1007/s00414-013-0890-z

Mjor, I. A., & Fejerskov, O. (Eds.). (1986). *Human Oral Embriology and Histology*. Munksgaard.

Moore, W. J., & Corbett, E. (1973). The distribution of dental caries in ancient British populations. *Caries Research*, *7*(2), 139–153. https://doi.org/10.1159/000259838

Nelson, E. A., Halling, C. L., & Buikstra, J. E. (2019). Evidence of skeletal fluorosis at the ray site, Illinois, USA: a pathological assessment and discussion of environmental factors. *International Journal of Paleopathology*, *26*, 48–60. https://doi.org/10.1016/j.ijpp.2019.05.003

Norén, J. G. (1984). Microscopic study of enamel defects in deciduous teeth of infants of diabetic mothers. *Acta Odontologica Scandinavica*, *42*(3), 153–156. https://doi.org/10.3109/00016358408993866

Oliveira, A. F. B., Chaves, A. M. B., & Rosenblatt, A. (2006). The influence of enamel defects on the development of early childhood caries in a population with low socioeconomic status: A longitudinal study. *Caries Research*, *40*(4), 296–302. https://doi.org/10.1159/000093188

O'Sullivan, A., Sonia, B., Williams, A., & Curzon, M. E. J. (1992). Dental caries in relation to nutritional stress in early English child populations. *Pediatric Dentistry*, *14*(1), 26–29.

Pitre, M. C., Stark, R. J., & Gatto, M. C. (2016). First probable case of scurvy in ancient Egypt at Nag el-Qarmila, Aswan. *International Journal of Paleopathology*, *13*, 11–19. https://doi.org/10.1016/j.ijpp.2015.12.003

Reed, S. G., Voronca, D., Wingate, J. S., Murali, M., Lawson, A. B., Hulsey, T. C., Ebeling, M. D., Hollis, B. W., & Wagner, C. L. (2017). Prenatal vitamin D and enamel hypoplasia in human primary maxillary central incisors: a pilot study. *Pediatric Dental Journal*, *27*(1), 21–28. https://doi.org/10.1016/j.pdj.2016.08.001

Ripa, L. W. (1988). Nursing caries: a comprehensive review. *Pediatric Dental Journal*, *10*(4), 268–282.

Schroth, R. J., Dhalla, S., Tate, R., & Moffatt, M. E. K. (2021). Prenatal and early childhood determinants of enamel hypoplasia in infants. *Journal of Pediatrics, Perinatology and Child Health*, *5*(1), 5–17. https://doi.org/10.26502/jppch.74050058

Schuurs, A. (2013). *Pathology of the Hard Dental Tissues*. John Wiley & Sons, Ltd.

Seow, W. (2014). Developmental defects of enamel and dentin: challenges for basic science research and clinical management. *Australian Dental Journal*, *59*, 143–154. https://doi.org/10.1111/adj.12104

Snoddy, A. M. E., Buckley, H. R., Elliott, G. E., Standen, V. G., Arriaza, B. T., & Halcrow, S. E. (2018). Macroscopic features of scurvy in human skeletal remains: a literature synthesis and diagnostic guide. *American Journal of Physical Anthropology*, *167*(4), 876–895. https://doi.org/10.1002/ajpa.23699

Subramaniam, P., Gupta, T., & Sharma, A. (2016). Prevalence of molar incisor hypomineralization in 7–9-year-old children of Bengaluru City, India. *Contemporary Clinical Dentistry*, *7*(1), 11–15. https://doi.org/10.4103/0976-237X.177091

Suga, S. (1989). Enamel hypomineralization viewed from the pattern of progressive mineralization of human and monkey developing enamel. *Advances in Dental Research*, *3*(2), 188–198. https://doi.org/10.1177/08959374890030021901

Velló, M., Martínez-Costa, C., Catalá, M., Fons, J., Brines, J., & Guijarro-Martínez, R. (2010). Prenatal and neonatal risk factors for the development of enamel defects in low birth weight children. *Oral Diseases*, *16*(3), 257–262. https://doi.org/10.1111/j.1601-0825.2009.01629.x

Walker, D. (2012). *Disease in London, 1st-19th Centuries: An Illustrated Guide to Diagnosis*. MoLA Monograph.

Walker, P. L., Bathurst, R. R., Richman, R., Gjerdrum, T., & Andrushko, V. A. (2009). The causes of porotic hyperostosis and cribra orbitalia: a reappraisal of the iron-deficiency-anemia hypothesis. *American Journal of Physical Anthropology*, *139*(2), 109–125. https://doi.org/10.1002/ajpa.21031

Warren, J. J., Levy, S. M., & Kanellis, M. J. (2001). Prevalence of dental fluorosis in the primary dentition. *Journal of Public Health Dentistry*, *61*(2), 87–91. https://doi.org/10.1111/j.1752-7325.2001.tb03371.x

Wasterlain, S. N., & Dias, G. J. (2009). Amelogenesis imperfecta in an early 20th century population from central Portugal. *International Journal of Osteoarchaeology*, *19*(3), 424–435. https://doi.org/10.1002/oa.972

Weerheijm, K. L., Jälevik, B., & Alaluusua, S. (2001). Molar-incisor hypomineralisation. *Caries Research*, *35*, 390–391. https://doi.org/10.1159/000047479

How to cite this article: Tesi, C., Ricci, S., Levrini, L., Giorgetti, G., Campagnolo, M., Ciliberti, R., Fusco, R., Larentis, O., & Licata, M. (2023). Defects-related early childhood caries as hints of possible maternal–fetal health issues: Evidence from medieval northern Italy. *International Journal of Osteoarchaeology*, 1–20. https://doi.org/10.1002/oa.3206